Dielectric, elastic, piezoelectric, electro-optic, and elasto-optic tensors of $BaTiO_3$ crystals

M. Zgonik, P. Bernasconi, M. Duelli, R. Schlesser, and P. Günter
Institute of Quantum Electronics, Swiss Federal Institute of Technology, ETH Hönggerberg, CH-8093 Zürich, Switzerland

M. H. Garrett and D. Rytz
Sandoz Huningue, S.A., Centre de Recherche en Optoélectronique, Bât. 195/04, Av. de Bâle, F-68330 Huningue, France

Y. Zhu and X. Wu
Institute of Physics, Chinese Academy of Sciences, P.O. Box 603, Beijing 100080, China
(Received 1 March 1994)

The complete set of material parameters of a top-seeded solution-grown $BaTiO_3$ crystal has been determined by numerically evaluating available measurements and using additional measurements presented in this work. The parameters were determined at room temperature and consist of the low-frequency clamped dielectric constants ϵ_{ij}^S, elastic stiffness constants at constant electric field c_{ijkl}^E, piezoelectric stress coefficients e_{ijk}, elasto-optic tensor at constant electric field p_{ijkl}^E, and clamped electro-optic coefficients r_{ijk}^S.

I. INTRODUCTION

Oxygen octahedra ferroelectrics are important materials because of their electro-optic and nonlinear-optic as well as acoustic and acousto-optic properties.[1] Crystals with the simplest structure in this group of materials belong to the perovskite class, with $SrTiO_3$, $BaTiO_3$, and $KNbO_3$ the most widely studied members. The latter two crystals are especially interesting for nonlinear-optical applications because of their large values of spontaneous polarization at room temperature and the high packing density of oxygen octahedra. They undergo a series of phase transitions from the high-temperature cubic phase to the tetragonal, orthorhombic, and to the low-temperature rhombohedral phase.

Barium titanate is an extensively used photorefractive material because of the large electro-optic coefficients.[2,3] In recent papers the necessity of considering the elasto-optic contribution to the refractive index changes in photorefractive experiments was pointed out.[4–6] Besides the refractive indices and the clamped (strain-free) electro-optic coefficients r_{ijk}^S, the piezoelectric stress tensor e_{ijk}, the elasto-optic (Pockels) tensor at constant electric field p_{ijkl}^E, and the tensor of the elastic constants at constant electric field c_{ijkl}^E must be known in order to calculate effective electro-optic coefficients[6] that describe the optical indicatrix changes under the influence of the electric field grating. Unfortunately, the material properties of most photorefractive crystals which are necessary in order to evaluate the refractive index changes have not been known completely. Only recently has a complete set of material constants of $KNbO_3$ crystal been determined.[7]

In this paper we will focus on the room-temperature elastic, elasto-optic, dielectric, piezoelectric, and electro-optic properties of tetragonal $BaTiO_3$ crystals. We first review the published data and present our measurements of material responses. From this information the complete set of material parameters is extracted by a fitting procedure.

II. OVERVIEW OF PUBLISHED DATA AND ADDITIONAL MEASUREMENTS

The point group symmetry of tetragonal $BaTiO_3$ is $4mm$ and we use a coordinate system with axes x, y, and z aligned along the crystallographic axes a_1, a_2, and c. The tetragonal c axis is parallel to the spontaneous polarization; therefore the positive direction of z is the direction of the electric field used to pole the crystal.

In describing the response of a piezoelectric crystal to external electrical and mechanical fields one can choose different sets of independent variables.[8] Each set consists of one mechanical variable (stress or strain) and one electrical (electric field strength or electric displacement) variable. The materials constants describing the response in each of these sets depend on the selection of independent variables. The elastic and dielectric response in two different sets is given as[8]

$$T_{ij} = c_{ijkl}^E S_{kl} - e_{kij} E_k, \tag{1}$$

$$D_i = e_{ijk} S_{jk} + \epsilon_0 \epsilon_{ij}^S E_j, \tag{2}$$

and

$$S_{ij} = s_{ijkl}^E T_{kl} + d_{kij} E_k, \tag{3}$$

$$D_i = d_{ijk} T_{jk} + \epsilon_0 \epsilon_{ij}^T E_j. \tag{4}$$

Summation over repeated indices is assumed throughout this paper. The set of independent variables in (1) and

 ©1994 The American Physical Society

(2) consists of the elastic strain tensor S_{kl} and the vector of the electric field strength E_i, while for (3) and (4) the elastic stress tensor T_{kl} is used instead of S_{kl}. The dielectric response is given by the clamped (zero strain) dielectric constant ϵ_{ij}^S in the first case and by the unclamped (zero stress) dielectric constant ϵ_{ij}^T in the second case. The tensors c_{ijkl}^E and s_{ijkl}^E are the elastic stiffness and compliance tensors at $E = 0$, while e_{kij} and d_{kij} are the piezoelectric stress and strain tensors, respectively. Materials constants in different sets can be related through thermodynamic reasoning.[8] Here we give three relations that will be used later. They are

$$c_{ijkl}^D - c_{ijkl}^E = e_{mij}e_{nkl}/(\epsilon_0\epsilon_{mn}^S), \tag{5}$$

$$\epsilon_0(\epsilon_{ii}^T - \epsilon_{ii}^S) = e_{ilm}d_{ilm}, \tag{6}$$

and

$$e_{ijk} = c_{lmjk}^E d_{ilm}. \tag{7}$$

Previously measured materials constants of $BaTiO_3$ are reviewed in this section. We have also performed several additional experiments in order to complete the data sets. In addition, improvements in the accuracy of some earlier data could be obtained because of the improved optical quality and larger size of the crystal samples that are available nowadays.

The crystals we used in this work were all nominally undoped top seeded solution grown and were produced at the Massachusetts Institute of Technology, Cambridge; at Sandoz Optoelectronique, Huningue; and at the Institute of Physics, Chinese Academy of Sciences, Beijing. The samples were light yellow in color and were all carefully poled to be single domain. Only the best samples were selected for the measurements.

A. Dielectric, elastic, and piezoelectric measurements

The complete data set on dielectric, elastic, and piezoelectric properties of $BaTiO_3$ at room temperature was first determined by Berlincourt and Jaffe[9] and later in the whole tetragonal phase by Schaefer *et al.*[10] Top-seeded solution-grown crystals used for the measurements published in 1986 (Ref. 10) are of better quality than the previously investigated crystals[9] grown by the Remeika method.[11] The two published sets of data still agree rather well at room temperature but we consider only the later results. From Ref. 10 we see that a minimum number of different measurements was performed which allowed the determination of the whole set. Here we list the results of these measurements because only these (raw data) can be used in our evaluation.

We start with a discussion of dielectric constants which were recently determined also by Nakao *et al.*[12] We also measure the dielectric constants in a range from 100 Hz to 13 MHz as a test of the quality of every sample we investigate by using a HP-4192A impedance analyzer. We use evaporated gold or silver paste electrodes which give the same results within the experimental inaccuracy. The measured capacitances at low frequencies are constant over three decades from 100 Hz to 100 kHz, they show mechanical resonances in the range from 100 kHz to a few MHz, and are constant at higher frequencies, where the crystal can be considered to be mechanically clamped. The ratio between the free (low-frequency) and the clamped (high-frequency) values of the dielectric constant was taken as a gauge of the quality of the single-domain state of the crystal as discussed in Ref. 12. Only the crystals satisfying this criterion were used for further studies. Therefore all our measurements were performed on crystals free from 180° domains.

The values for ϵ_{33} obtained in different groups are quite consistent and are $\epsilon_{33}^T = 130 \pm 5$ for the free dielectric constant and $\epsilon_{33}^S = 56 \pm 3$ for the clamped. The values of ϵ_{11} vary more from crystal to crystal because this dielectric tensor component diverges when approaching the phase transition from the tetragonal to the orthorhombic phase, normally taking place at 6 °C. Small variations in the phase transition temperature in different samples also affect the values of this dielectric constant at room temperature. Taking an average over all available data measured at 23 °C and being a little conservative in inaccuracy estimation we determine the free and the clamped dielectric constants perpendicular to the polar axis to be $\epsilon_{11}^T = 4400 \pm 400$ and $\epsilon_{11}^S = 2180 \pm 300$. These values are also listed in Table I where we collect all the measured quantities that we consider in our work.

From the resonance frequencies of differently cut samples three components of the elastic compliance tensors, s_{1111}^E, s_{3333}^D, and s_{1313}^E, were determined.[10] Three further results of resonance measurements[10] are expressed as a linear combination of several components of the elastic compliance tensor. The measured quantities and the results are listed in lines 5–10 in Table I.

Additional data on the elastic properties of $BaTiO_3$ at room temperature were measured by Ishidate and Sasaki.[13] They investigated spectra of Brillouin scattered light and determined the following elastic stiffness constants: c_{1111}^E, c_{1313}^E, c_{3333}^D, c_{1313}^D, and c_{1212}. Their values are listed in lines 11–15 in Table I. Because of an error in their analysis of the angular dependence of the sound velocities of the two acoustic waves which propagate in the plane (010) and are polarized in this plane, we use their velocity data here. The velocities of these two waves propagating along the [101] direction are given by

$$\rho \begin{Bmatrix} v_{\mathrm{QL}}^2 \\ v_{\mathrm{QT}}^2 \end{Bmatrix} = A + B \begin{Bmatrix} + \\ - \end{Bmatrix} \sqrt{(A-B)^2 + 4C^2}, \tag{8}$$

with QL standing for quasilongitudinal and QT for quasitransverse polarization. The crystal mass density $\rho = 6020\ \mathrm{kg\,m^{-3}}$, and the coefficients A, B, and C that appear above are expressed with the elastic stiffness constants, with piezoelectric stress coefficients e_{ijk}, and with clamped dielectric constants as

$$A = c_{1111}^E + c_{1313}^E + (e_{311} + e_{131})^2/[\epsilon_0(\epsilon_{11}^S + \epsilon_{33}^S)], \tag{9}$$

$$B = c_{3333}^E + c_{1313}^E + (e_{333} + e_{131})^2/[\epsilon_0(\epsilon_{11}^S + \epsilon_{33}^S)], \tag{10}$$

and

$$C = c^E_{1133} + c^E_{1313} + \frac{(e_{333} + e_{131})(e_{311} + e_{131})}{\epsilon_0(\epsilon^S_{11} + \epsilon^S_{33})}. \quad (11)$$

From the measured velocities[13] v_{QL}= 6800 m s^{-1} and v_{QT} = 2500 m s^{-1} the values for the quantities ρv^2_{QL} and ρv^2_{QT} were calculated and are listed in lines 16 and 17 of Table I.

Plate resonance measurements mentioned above and additional dielectric measurements were used in the past to determine the piezoelectric coefficients. In our Table I, in lines 18 and 19, we have included two additional measurements[10] that give the ratio $d^2_{311}/(s^E_{1111}\epsilon_0)$ and the square of the piezoelectric coupling constant k^2_{33}.

Optical interferometry was used by Ducharme *et al.*[14] to determine the piezoelectric coefficient d_{311}. Their value of +28.7 pm/V, however, is not included in Table I. Their positive sign is in contradiction with all other results[9,10] and also with the dependence of the lattice constant a on the spontaneous polarization. The dielectric (spontaneous) polarization is the principal driving term of crystal modifications in the ferroelectric phase. An increase of the dielectric polarization—achieved either by reducing the temperature or by applying an electric field parallel to the original poling field—results in a reduction of the lattice constant a.[15]

We have repeated the interferometric measurements of the signs and of the values of the two piezoelectric strain coefficients d_{333} and d_{311}. We used two samples for these measurements with evaporated gold electrodes on the c surfaces. The samples were block shaped with typical dimensions of 5 mm. A difference from the measurement performed by Ducharme *et al.*[14] was that we glued one of the sample surfaces on a thick glass plate which was fixed in a mirror mount. The light beam was reflected from the other surface only and interfered with the beam from the second arm of the Michelson interferometer. In

TABLE I. Measurements used in the evaluation of material constants of top-seeded solution-grown $BaTiO_3$ crystals.

	Measured quantity	Reference	Measured value	Fitted value	Units
1	ϵ^T_{11}	10, 12, this work	4400±400	4380	
2	ϵ^T_{33}	10, 12, this work	130±5	129	
3	ϵ^S_{11}	12, this work	2180±300	2200	
4	ϵ^S_{33}	12, this work	56±3	56	
5	s^E_{1111}	10	7.35±0.02[a,b]	7.37	10^{-12} m^2 N^{-1}
6	s^D_{3333}	10	10.0±0.07[a,c]	5.6	10^{-12} m^2 N^{-1}
7	s^E_{1313}	10	4.55±0.02[a,b]	4.11	10^{-12} m^2 N^{-1}
8	$0.5s^E_{1111} + 0.5s^E_{1122} + 0.25s_{1212}$	10	5.06±0.05[a,b]	4.86	10^{-12} m^2 N^{-1}
9	$0.78s^E_{1111} + 0.01s^E_{3333} + 0.21s^E_{1133} + 0.105s^E_{1313}$	10	6.76±0.06[a,b]	6.7	10^{-12} m^2 N^{-1}
10	$(s^E_{1111} + s^E_{1122})/[1 + 0.19s^E_{1122}/(s^E_{1111} - s^E_{1122})]$	10	6.13±0.06[a,b]	6.17	10^{-12} m^2 N^{-1}
11	c^E_{1111}	13	22.3 ± 1	22.2	10^{10} N m^{-2}
12	$c^D_{3333} = c^E_{3333} + e^2_{333}/\epsilon_0\epsilon^S_{33}$	13	24.0 ± 1	24.0	10^{10} N m^{-2}
13	c^E_{1313}	13	6.2 ± 0.3	6.1	10^{10} N m^{-2}
14	$c^D_{1313} = c^E_{1313} + e^2_{131}/\epsilon_0\epsilon^S_{11}$	13	12.1 ± 0.5	12.1	10^{10} N m^{-2}
15	c_{1212}	13	13.4 ± 0.6	13.4	10^{10} N m^{-2}
16	ρv^2_{QL}	13	27.8 ± 1.5	28.0	10^{10} N m^{-2}
17	ρv^2_{QT}	13	3.8 ± 0.2	3.8	10^{10} N m^{-2}
18	$d^2_{311}/(s^E_{1111}\epsilon_0)$	10	17.1±0.1[a,b]	17.1	
19	$k^2_{33} = d^2_{3333}/(\epsilon_0\epsilon^T_{33}s^E_{3333})$	10	0.303[a,c]	0.54	
20	d_{311}	this work	−32.5±2	−33.4	10^{-12} C N^{-1}
21	d_{333}	this work	90±5	90	10^{-12} C N^{-1}
22	$(p^E_{1111})^2$	this work	0.24±0.03	0.25	
23	$(p^E_{1111}/p^E_{2211})^2$	this work	22.6±2	22.5	
24	$(p^E_{1111}/p^E_{3311})^2$	this work	52±5	52	
25	$(p^*_{3333})^2 = (p^E_{3333} - r^S_{333}e_{333}/\epsilon_0\epsilon^S_{33})^2$	this work	0.055±0.01	0.055	
26	$(p^*_{3333}/p^*_{1133})^2$	this work	13.6±2	13.6	
27	$r^T_{113} - 2(n_a - 1.5)d_{311}/n^3_a$	this work, 14, 23	11.2±1.3	12.1	10^{-12} m V^{-1}
28	$r^T_{333} - 2(n_c - 1.5)d_{311}/n^3_c$	this work, 23	113±5	110	10^{-12} m V^{-1}
29	r^T_{131}	this work, 23	1300±150	1300	10^{-12} m V^{-1}
30	$r^S_{113}/[r^T_{113} - 2(n_a - 1.5)d_{311}/n^3_a]$	this work	0.83±0.07	0.84	
31	$r^S_{333}/[r^T_{333} - 2(n_c - 1.5)d_{311}/n^3_c]$	this work	0.38±0.03	0.37	
32	r^S_{131}/r^T_{131}	this work	0.56±0.05	0.56	
33	$r^{eff}_{33}/r^{eff}_{11}$	14, 24	3.6±0.2	3.7	

[a] Experimental accuracies were not given in the original publication but have been communicated by H. Schmitt, Universität des Saarlandes, Saarbrücken, Germany.

[b] 10% standard deviations were used in the fitting procedure.

[c] These two measurements are not used as constraints in the final fitting procedure because of large discrepancy with the results of the fit. For both measurements the same, possibly incompletely poled sample was used.

the case of measurement of d_{333} the sample was glued with the silver paste and the light was reflected from the other gold electrode. For the measurement of d_{311} one a_1 sample surface was painted black and then glued onto the support with optical cement. The other a_1 surface of the sample was used as the mirror inside the interferometer. Measurements were performed at different frequencies in the range from 10 Hz to 50 kHz to check and eliminate the possible contributions of mechanical resonances of the sample support. The results for $d_{311} = (-32.5 \pm 2)$ pm/V and $d_{333} = (+90 \pm 5)$ pm/V are included in Table I. The absolute value of the d_{311} is quite close to the previous result 28.7 pm/V.[14] The signs agree with the temperature dependence of the lattice constants. The negative sign of d_{311} was also confirmed later in our electro-optic measurement as explained in the next subsection.

B. Elasto-optic and electro-optic measurements

Material tensors of $BaTiO_3$ which are important for electro-optical and acousto-optical applications are r_{ijk}, the electro-optic coefficients, and p_{ijkl}, the elasto-optic coefficients. The elasto-optic coefficients p_{ijkl} of $BaTiO_3$ crystal were determined in the cubic phase between 131 °C and 170 °C by Cohen *et al.*[16] In the tetragonal phase, however, they have not been determined up to now to our knowledge.

For the measurements of this tensor we used the Dixon and Cohen method[17] which consists of a measurement of diffraction of light off the gratings produced by pulses of ultrasonic waves. We send a pulse of longitudinally polarized ultrasonic waves through a reference material, which is a slab of fused silica, and through the $BaTiO_3$ sample which is attached with benzophenone at the end of the reference material.[7] The ultrasonic pulse is partially reflected from the interface between the two materials and from the end face of the sample. The measurements are performed in two block-shaped samples with all the surfaces optically polished. Both samples with all the edges longer than 5.5 mm are large enough to avoid overlap of the light pulses diffracted off the counterpropagating ultrasonic pulses.

The data on $BaTiO_3$ which are necessary to evaluate these measurements are the sound velocity with the values 6100 m s^{-1} and 6300 m s^{-1} for the waves propagating along the a and c crystallographic axes, and the refractive indices[18] are $n_a = 2.412$ and $n_c = 2.360$ for the light polarized along the a and c axes, respectively.

In the case of purely longitudinal waves propagating along the crystallographic axes of $BaTiO_3$ the change of the inverse of the dielectric constant at optical frequencies is given as

$$\Delta\left(\frac{1}{n^2}\right)_{ii} = r^S_{iik}E_k + p^E_{iill}S_{ll}, \tag{12}$$

with r^S_{iik} the electro-optic strain-free coefficients, p^E_{iill} the elasto-optic coefficients at constant electric field, and the elastic deformation described by the symmetrized strain tensor S_{kl}. A longitudinal sound wave propagating along the x axis induces no electric field in the crystal. Therefore three components of the elasto-optic tensor at zero electric field can be determined directly. We have first determined the absolute value of the coefficient p^E_{1111} by sending a light beam through the crystal along the z and also along the y direction. The light polarization in these measurements was along the x axis. The other two coefficient, p^E_{2211} and p^E_{3311}, were measured relatively to p^E_{1111}. The values are listed in lines 22–24 of Table I.

With the sound wave propagating along the z axis a longitudinal electric field is generated because of the piezoelectric coupling through the e_{333} tensor element.[19] In this case one measures the effective elasto-optic tensor components p^*_{ii33}. They are related to the elasto-optic tensor at zero electric field by

$$p^*_{ii33} = p^E_{ii33} - \frac{r^S_{ii3}e_{333}}{\epsilon_0\epsilon^S_{33}}. \tag{13}$$

The measurements with the sound propagation along the z axis appeared to be more difficult because of the apparently higher absorption of the ultrasound in this direction or stronger influence of crystal inhomogeneities. More measurements were done to determine these two coefficients p^*_{1133} and p^*_{3333}. The absolute value of p^*_{3333} was first determined and the relative measurement of both coefficients was repeated many times. The values are included in Table I in lines 25 and 26.

In the case of electro-optic measurements the available data are more numerous but no recent measurements of the clamped values have been reported and the only available data are almost thirty years old.[20,21] There are three recent sources of data on the stress-free coefficients: Ducharme *et al.*,[14] Jullien *et al.*,[22,23] and Holtmann.[24] All recent data were obtained by interferometric techniques.

The total optical phase change of an optical beam $\Delta\Phi$ in a crystal subjected to an external electric field is

$$\Delta\Phi = \Delta\left[\frac{2\pi}{\lambda_0}(n_i - n_0)L\right] = \frac{2\pi}{\lambda_0}\left[L\Delta n_i + (n_i - n_0)\Delta L\right], \tag{14}$$

where n_i is the refractive index of the crystal, n_0 is the refractive index of the surrounding medium (air or index-matching liquid), and λ_0 is the wavelength of light in vacuum. L is the length of the geometrical path of the beam inside the crystal. Both n_i and L change in general under the influence of the electric field. Ducharme *et al.*[14] separated both contributions in their electro-optic measurements. In the case of an electric field E_3, with a frequency below the piezoelectric resonances of the $BaTiO_3$ sample, applied along the z axis the total optical phase change for a beam propagating along the a_1 axis can be written as

$$\Delta\Phi = -\frac{\pi}{\lambda_0}n_i^3\left[r^T_{ii3} - \frac{2(n_i - n_0)}{n_i^3}d_{311}\right]L_aE_3, \tag{15}$$

where n_i can be either the refractive index n_a or n_c, depending on the beam polarization, r^T_{ii3} the appropriate unclamped electro-optic coefficient, d_{311} the piezoelectric

strain coefficient, and L_a the length of the crystal along the a_1 axis. The effect of the index-matching liquid, if used, is to reduce the piezoelectric contribution as seen from Eq. (15).

As mentioned before, the sign of d_{311} determined in Ref. 14 and used in the evaluation of the interferometric measurements in Refs. 14 and 24 was wrong. When one uses the positive value of $d_{311} = +28.7$ pm/V, the piezoelectric contribution to the measured electro-optic coefficient—the second term inside the brackets of Eq. (15)—is calculated to be negative. For the crystal in air this contribution amounts to approximately -5.9 pm/V.

New experiments to remeasure the signs and also the values of all the EO coefficients seemed to be necessary. We first carried out an evaluation of the stress-free electro-optic coefficients r^T_{113} and r^T_{333} at a wavelength of 633 nm.

A Michelson interferometer was used with the crystal placed inside one of the arms. The crystal is immersed in a cuvette with index-matching oil with an index of refraction $n = 1.5$ to reduce Fresnel reflection at the surfaces and to reduce the influence of the piezoelectric contributions. The beam propagates along one a crystal axis. An ac field (amplitude 1–10 V/cm) at several frequencies (10^2–10^5 Hz) is applied to the $BaTiO_3$ probe along the c axis. A photodiode with a broadband amplifier (dc, 100 MHz) is used to measure the light intensity behind a pinhole which selects a small part of the interference pattern. The phase difference Φ between the two interfering waves is adjusted to be exactly $\pi/2$ (modulo 2π). The applied field on the crystal induces small-amplitude ($\Delta\Phi \ll 1$) phase changes of one wave which in turn generate intensity oscillations in the interference pattern whose amplitude δI is given by

$$\frac{\delta I}{\Delta I} = -\frac{1}{2}\Delta\Phi, \tag{16}$$

where ΔI is the difference between maximum and minimum intensity reached by the interference by changing the phase Φ from $2m\pi$ to $(2m+1)\pi$, where m is an arbitrary integer. The signal is then fed to a lock-in amplifier from where we get the amplitude of the light intensity oscillations in phase with the applied field. By selecting the light polarization perpendicular and parallel to the c axis the value of the expression in the square bracket of Eq. (15) is determined for $i = 1$ and 3, respectively. These values are included in Table I in lines 27 and 28.

The signs of both terms in Eq. (15) were determined to be equal and positive. To double-check the sign of the piezoelectric contribution, the measurements described above were performed also with the crystal in air, because the piezoelectric contribution is proportional to $n_{\text{crystal}} - n_{\text{surrounding}}$. Light polarization along x was selected in order to decrease the first term in Eq. (15). In this way we increased the relative importance of the second term. Consistently larger values than the one reported in line 27, Table I, were measured in this case, demonstrating that both terms in Eq. (15) have the same sign and therefore proving that $d_{311} < 0$.

We can compare our results with the measurements of Ducharme *et al.*[14] if we subtract the piezoelectric contribution of -5.9 pm/V from their results for r^T_{113} and r^T_{333}. The value of $r^T_{113} - 5.9$ pm/V $= 13.6$ pm/V agrees with our measurements performed in air to within 5%. Their measured value for r^T_{333} is 20% lower than ours. Jullien *et al.*[23] published their values for r^T_{113} and r^T_{333} without subtracting the piezoelectric contribution. Their value for $r^T_{113} = 12$ pm/V corresponds to our raw measurement within the experimental inaccuracy. Their values for the other coefficient in undoped crystals are more scattered; however, the average value of 115 pm/V lies very close to our result.

The measurement of the so-called off-diagonal element of the electro-optic tensor r^T_{131} was carried out by measuring the field-induced birefringence. An ac field is applied along the a_1 axis of the crystal and the beam enters the crystal through the c surface, propagating in the c-a_1 plane. The internal angle between the beam propagation direction and the c axis is α. The light entering the crystal is polarized at 45° from the incidence plane to have the intensities of the two eigenpolarizations inside the crystal approximately equal. The phase difference $\Delta\Phi$ between the two light components, one polarized parallel to a_2, the other lying in the a_1-c plane, is then detected by a crossed analyzer in front of the same phase-sensitive detection system previously described. The phase difference is given by the following formula:

$$\Delta\Phi = -\frac{\pi n_e^3}{\lambda_0}\left[2r^T_{131}\cos\alpha\sin\alpha - \frac{2(n_e - n_a)}{n_e^3}d_{\text{eff}}\right] \times \frac{L_c}{\cos\alpha}E_1, \tag{17}$$

where n_e is the index of refraction for the extraordinary polarization $n_e = n_a n_c/\sqrt{n_c^2\cos^2\alpha + n_a^2\sin^2\alpha}$, n_a is the ordinary refractive index, r^T_{131} is the coefficient we want to measure, L_c is the length of the crystal along the c direction, and d_{eff} is an effective piezoelectric coefficient which depends on d_{131} and on the mechanical mounting of the crystal. Because of the small difference between the refractive indices, the piezoelectric contribution can be neglected, which we tested by mounting the crystal in different ways and performing the measurements with different frequencies and propagation angles. Our value of $r^T_{131} = (1300 \pm 150)$ pm/V—included in Table I—lies within the experimental inaccuracies of the published data.[23]

A second method to determine simultaneously both clamped and unclamped electro-optic coefficients consisted in applying the field in the form of a square wave (amplitude 2–20 V/cm, frequency 500 Hz) with short rise time (≤ 10 ns) instead of using sine waves.[21] The same Michelson interferometer and the single-beam interference configurations as described before were used in the measurements. But in this case the measurement of δI was not taken from the lock-in but was directly read with a digital oscilloscope, typically averaging the signal over 1000 pulses.

When a steplike electric field is applied to the crystal the electro-optic response of the bound electrons and optical phonons shows up instantaneously on a nanosec-

ond time scale. The electro-optic response due to the piezoelectric contribution, however, is delayed. The crystal starts ringing in its mechanical resonances which are clearly seen in Fig. 1. These resonances are finally damped in approximately 0.1 ms and the crystal is in a completely stress-free (unclamped) state. As seen in the figure, both regimes can be distinguished rather well. The first step in the response gives the clamped value of the electro-optic coefficient while the free value of the electro-optic coefficient with the piezoelectric contribution included is given by the value at longer times. With this technique we determined the ratios between the clamped and the free response and we include these data in Table I, lines 30–32. The electro-optic response of the free crystal was also absolutely determined with this technique. It gave us the same results within the experimental inaccuracy as the ac modulation method.

There is another measurement that we include in Table I that is related to the photorefractive applications of $BaTiO_3$. When the photorefractive grating vector is aligned along the z axis the effective electro-optic tensor is given by[6,7]

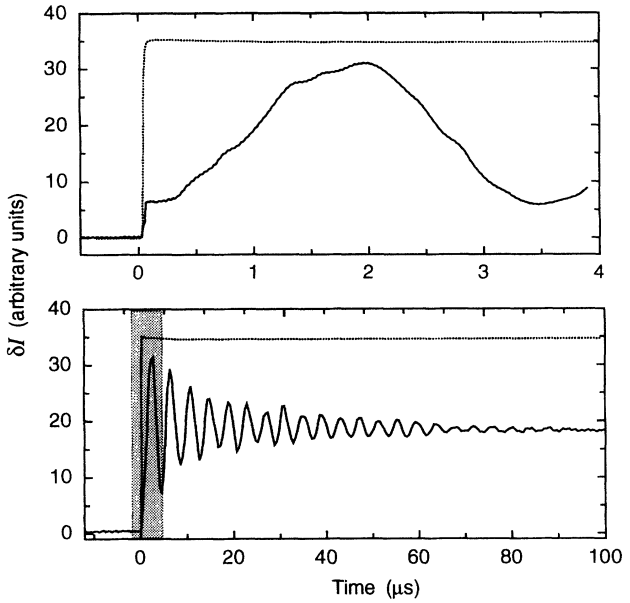

FIG. 1. Intensity change δI (solid line) of the Michelson interferometer output due to the crystal response to a step change of the applied field (dotted line with independent scale). The upper curve shows the measurement in the first few microseconds, the first step of the curve corresponding to the electro-optic response of a clamped crystal. Evolution of the signal at later times is presented in the lower picture. The oscillations show the damped mechanical resonances of the crystal. The stationary value reached after approximately 100 μs corresponds to the unclamped equilibrium state of the crystal. The curve shown was taken with the electric field E_3 and the light polarization along the c axis. The quotient between the first step and the stationary value gives in this case the ratio $r^S_{333}/[r^T_{333} - 2(n_c - 1.5)d_{311}/n_c^3]$.

$$r_{ii}^{\text{eff}} = r_{ii3}^S + \frac{p_{ii33}^E e_{333}}{c_{3333}^E}, \tag{18}$$

where the index i takes the value of 1 or 3. The ratio between the two components of this tensor $r_{33}^{\text{eff}}/r_{11}^{\text{eff}}$ can be measured relatively precisely in beam-coupling or diffraction experiments when the fringe spacing of the photorefractive grating is large so that beam polarization is approximately parallel to the z axis when using extraordinary polarized beams. The measured ratios of 3.56 in Ref. 14 and 3.7 in Ref. 24 lie within the experimental inaccuracy of each other. The value of 3.6 with an estimated inaccuracy of 0.2 is included in Table I.

III. DETERMINATION OF THE COMPLETE SET OF MATERIALS PARAMETERS

To analyse the set of measured data and to determine the values of all the material constants we resort to a least-squares fit approach. Each experimental result with its estimated uncertainty represents a constraint on the values of the material parameters. The constraint is expressed as an algebraic relationship involving some fundamental physical constants and a subset of the whole set of independent material parameters. As the complete set of independent material tensors describing the mixed dielectric, elastic, and optical properties, we have selected ϵ_{ii}^S, c_{ijkl}^E, e_{ijk}, r_{ijk}^S, and p_{ijkl}^E, that is, the applied electric field strength E_i and the crystal deformation S_{ij} are the independent variables. The material response is then calculated by the strain-free (clamped) dielectric constants and EO coefficients, by the zero electric field elastic stiffness constants and elasto-optic coefficients, and by piezoelectric stress coefficients. The values of the parameters that were measured in stress-free conditions and the parameters evaluated at constant dielectric displacement were also treated in the numerical procedure by expressing them in terms of the basic set.

A. Determination of the constraints

The set of all constraints is given by equations of the form

$$f_i(a_1 \cdots a_n) = y_i, \; i = 1 \cdots k, \tag{19}$$

where y_i is the value of f_i that was determined in the experiment number i and $a_1 \cdots a_n$ is the complete set of n material parameters.

In the simplest case, where a material parameter was measured directly, the function $f_i(a_1 \cdots a_n)$ reduces to the value of one parameter a_j and the constraint has the simple form

$$a_j = y_i. \tag{20}$$

This is the case for the measurements listed in lines 3, 4, 11, 13, and 15 in Table I. To find the residual constraints we first solve Eq. (7) analytically to explicitly express the piezoelectric strain tensor in terms of the piezoelectric stress tensor e_{ijk} and the elastic constants c_{ijkl}^E to get

$$d_{311} = \frac{c^E_{3333}e_{311} - c^E_{1133}e_{333}}{(c^E_{1111} + c^E_{1122})c^E_{3333} - (c^E_{1133})^2}, \quad (21)$$

$$d_{333} = \frac{(c^E_{1111} + c^E_{1122})e_{333} - c^E_{1133}e_{311}}{(c^E_{1111} + c^E_{1122})c^E_{3333} - 2(c^E_{1133})^2}, \quad (22)$$

and

$$d_{131} = e_{131}/(2c^E_{1313}). \quad (23)$$

Expressions (21) and (22) define two additional constraints imposed by the measured values from lines 20 and 21 of Table I.

The analytical solutions for the d_{ijk} coefficients are introduced in relation (6) connecting the clamped and unclamped dielectric constants to get two constraints imposed by the measurements of the dielectric constants ϵ^T in a free crystal, lines 1 and 2 in Table I.

Elastic compliance tensors s_{ijkl} (E=0, and D=0) are expressed in terms of the elastic stiffness tensor c_{ijkl} through the following relations:

$$s^{E,D}_{1111} = \frac{(c^{E,D}_{1133})^2 - c^{E,D}_{1111}c^{E,D}_{3333}}{(c^{E,D}_{1111} - c^{E,D}_{1122})[2(c^{E,D}_{1133})^2 - c^{E,D}_{3333}(c^{E,D}_{1111} + c^{E,D}_{1122})]}, \quad (24)$$

$$s^{E,D}_{1122} = \frac{c^{E,D}_{1122}c^{E,D}_{3333} - (c^{E,D}_{1133})^2}{(c^{E,D}_{1111} - c^{E,D}_{1122})[2(c^{E,D}_{1133})^2 - c^{E,D}_{3333}(c^{E,D}_{1111} + c^{E,D}_{1122})]}, \quad (25)$$

$$s^{E,D}_{1133} = \frac{c^{E,D}_{1133}}{2(c^{E,D}_{1133})^2 - c^{E,D}_{3333}(c^{E,D}_{1111} + c^{E,D}_{1122})}, \quad (26)$$

$$s^{E,D}_{3333} = \frac{c^{E,D}_{1111} + c^{E,D}_{1122}}{2(c^{E,D}_{1133})^2 - c^{E,D}_{3333}(c^{E,D}_{1111} + c^{E,D}_{1122})}, \quad (27)$$

$$s_{1212} = 1/(4c_{1212}), \quad (28)$$

and

$$s^{E,D}_{1313} = 1/(4c^{E,D}_{1313}). \quad (29)$$

We then use the difference between the elements of the elastic stiffness tensor $c^D_{ijkl} - c^E_{ijkl}$ (5) to express all the residual acoustic and piezoelectric measurements (lines 5–19) with the basic set only.

The results of the elasto-optic measurements presented in lines 22–26 can be directly related to the basic set and give additional five constraints. In order to define the constraints by using the electro-optic measurements from lines 27–32 we insert the analytical solutions for the elements of the piezoelectric strain tensor (21)–(23) in the following relation

$$r^T_{ijk} = r^S_{ijk} + p^E_{ijlm}d_{klm}, \quad (30)$$

which connects the stress-free with the strain-free electro-optic coefficients. The last photorefractive measurement from line 33 is related to the basic set through Eq. (18) and completes the list of constraints.

B. Fitting

The number of constraints $k = 33$ is larger than the number of parameters $n = 20$; therefore it is possible to find the optimum values of the parameters that fulfill the set of constraints given in Table I by a least-squares procedure. The analysis was performed using a commercial application for numerical fitting on an Apple Macintosh computer.[25] The Levenberg-Marquardt algorithm is used which is described in Ref. 26. The algorithm finds the set of parameters that minimizes the sum χ^2 of the squared deviations of the function values $f_i(a_1 \cdots a_n)$ from the measured values y_i:

$$\chi^2 = \sum_i \frac{[f_i(a_1 \cdots a_n) - y_i]^2}{(\Delta y_i)^2}, \quad (31)$$

where Δy_i is the standard deviation of the data value y_i. The standard deviation Δy_i is generally assumed to be the inaccuracy of the data point y_i as given in Table I. The standard deviation can also be increased in order to reduce the weight of a particular measurement in the fit.

In order to determine the accuracies Δa_j of the parameter a_j a matrix G_{jk} is calculated from the standard deviation of the data points and from the partial deriva-

TABLE II. Basic set of the material parameters: dielectric (ϵ^S_{ij}), elastic stiffness (c^E_{ijkl}), piezoelectric stress (e_{ijk}), elasto-optic (p^E_{ijkl}), and clamped electro-optic (r^S_{ijk}) tensor elements of $BaTiO_3$ as determined by fitting the experimental data in Table I. All materials constants are given at room temperature (23 °C) at the wavelength $\lambda_0 = 633$ nm where the refractive indices are $n_a = 2.412$ and $n_c = 2.360$.

Parameter	Value	Accuracy	Units
ϵ^S_{11}	2200	±200	
ϵ^S_{33}	56	±3	
c^E_{1111}	222	±10	10^9 N m^{-2}
c^E_{1122}	108	±18	10^9 N m^{-2}
c^E_{1133}	111	±8	10^9 N m^{-2}
c^E_{3333}	151	±7	10^9 N m^{-2}
c^E_{1313}	61	±3	10^9 N m^{-2}
c_{1212}	134	±6	10^9 N m^{-2}
e_{311}	−0.7	±0.6	C m^{-2}
e_{333}	6.7	±0.3	C m^{-2}
e_{131}	34.2	±1.8	C m^{-2}
p^E_{1111}	0.50	±0.04	
p^E_{1122}	0.106	±0.01	
p^E_{1133}	0.20	±0.014	
p^E_{3311}	0.07	±0.007	
p^E_{3333}	0.77	±0.04	
p^E_{1313}	1.0	±0.2	
p^E_{1212} [a]			
r^S_{113}	10.2	±0.6	10^{-12} m V^{-1}
r^S_{333}	40.6	±2.5	10^{-12} m V^{-1}
r^S_{131}	730	±100	10^{-12} m V^{-1}

[a] The only missing value of the complete set: the elasto-optic tensor element p^E_{1212}, is less important for applications and could not be determined from the existing measurements. Other experimental methods or sample cuts will be necessary to determine it.

tives of the function with respect to the parameters as

$$G_{jk} = \sum_i \frac{1}{(\Delta y_i)^2} \frac{\partial f_i}{\partial a_j} \frac{\partial f_i}{\partial a_k}. \quad (32)$$

Then the so-called covariance matrix $\mathbf{M} = \mathbf{G}^{-1}$—the inverse of $\mathbf{G}$—is determined and the inaccuracy Δa_j is given as a diagonal element of the covariance matrix $\mathbf{M}$, that is, $\Delta a_j = M_{jj}$.

The numerical procedure was very stable and the results converged after only a few iterations. Two constraints, however, produced systematically large discrepancies of the fit. These two measurements—given in lines 6 and 19 of Table I—were made unimportant for the final fit by increasing their standard deviation to infinity. We believe that these two measurements which were performed in the same sample[10] are less reliable. The inaccuracy could be explained by the incomplete poling of the crystal and by the inaccuracy of the experimental method itself.[27]

The final set of parameters and the corresponding standard deviation obtained using our procedure are displayed in Table II. It is encouraging to note that all the other values obtained by the fitting procedure lie very close to the available measured values. Table III displays the calculated values of the additional material parameters derived from the basic set.

TABLE III. Additional material parameters of $BaTiO_3$ crystal: stress-free dielectric tensor ϵ_{ij}^T, elastic stiffness tensor at constant dielectric polarization c_{ijkl}^D, elastic compliance tensor at constant electric field s_{ijkl}^E, elastic compliance tensor at constant dielectric polarization s_{ijkl}^D, piezoelectric d_{ijk} tensor, and stress-free electro-optic tensor r_{ijk}^T. These materials constants are calculated from the basic set given in Table II, therefore also describing the properties at room temperature (23 °C) at the wavelength $\lambda_0 = 633$ nm.

Parameter	Value	Accuracy	Units
ϵ_{11}^T	4400	±400	
ϵ_{33}^T	129	±5	
c_{1111}^D	223	±10	10^9 N m^{-2}
c_{1122}^D	109	±5	10^9 N m^{-2}
c_{1133}^D	102	±5	10^9 N m^{-2}
c_{3333}^D	240	±10	10^9 N m^{-2}
c_{1313}^D	121	±5	10^9 N m^{-2}
s_{1111}^E	7.4	±0.3	10^{-12} m^2 N^{-1}
s_{3333}^E	13.1	±1.5	10^{-12} m^2 N^{-1}
s_{1122}^E	−1.4	±0.3	10^{-12} m^2 N^{-1}
s_{1133}^E	−4.4	±0.5	10^{-12} m^2 N^{-1}
s_{1212}[a]	1.9	±0.2	10^{-12} m^2 N^{-1}
s_{1313}^E[a]	4.1	±0.4	10^{-12} m^2 N^{-1}
s_{1111}^D	6.4	±0.3	10^{-12} m^2 N^{-1}
s_{3333}^D	5.6	±1	10^{-12} m^2 N^{-1}
s_{1122}^D	−2.3	±0.4	10^{-12} m^2 N^{-1}
s_{1133}^D	−1.7	±0.3	10^{-12} m^2 N^{-1}
s_{1313}^D[a]	2.1	±0.4	10^{-12} m^2 N^{-1}
d_{311}	−33.4	±2	10^{-12} C N^{-1}
d_{333}	90	±5	10^{-12} C N^{-1}
d_{131}[a]	282	±20	10^{-12} C N^{-1}
r_{113}^T	8	±2	10^{-12} m V^{-1}
r_{333}^T	105	±10	10^{-12} m V^{-1}
r_{131}^T	1300	±100	10^{-12} m V^{-1}

[a] Note that we strictly use the tensor notation which is much more practical than the matrix contracted notation and helps avoid errors in computer calculations. Factors of 4, $4s_{ijij} = s_{kk}$, and 2, $2d_{iji} = d_{ik}$, relate the above tensor elements to the matrix.

IV. CONCLUSIONS

Measurements on high-quality samples of top-seeded solution-grown crystalline $BaTiO_3$ have been performed in order to complete the set of data necessary to describe the optical response of this material to electric fields and elastic deformation. Improvements in the accuracy of some previously published results have been obtained because of better optical quality and larger size of the crystal samples that are available nowadays. The most important results are the values and the signs of the piezoelectric strain coefficients d_{311} and d_{333}, the absolute values of the elasto-optic coefficients, and all the electro-optic measurements. Both low-frequency electro-optic measurements in a stress-free sample and measurements in the inertia-clamped samples using a steplike electric field were used to correct the previous results. The complete set of materials parameters of the $BaTiO_3$ crystals at room temperature has been determined afterwards by a numerical fitting procedure. Each experimental result with its estimated uncertainty is used as a constraint on the values of the material parameters. The numerical procedure is very stable. The signs of the elasto-optic coefficients are also determined with great confidence. We propose that the calculated values presented in Table II be used as a consistent set of materials parameters of the $BaTiO_3$ crystal, in particular for describing its photorefractive properties, that is, to calculate its effective electro-optic and dielectric properties.

ACKNOWLEDGMENTS

We would like to thank Hans Schmitt, Steven Ducharme, Karsten Buse, Marc Fontana, and Roger Cudney for comments about the previous measurements on $BaTiO_3$ and for useful discussions. We are grateful to Ivan Biaggio for his expert help in numerical evaluation of the results by PROFIT[25] application.

[1] M. E. Lines and A. M. Glass, *Principles and Applications of Ferroelectrics and Related Materials* (Clarendon, Oxford, 1977).
[2] P. Günter, Phys. Rep. **93**, 199 (1982).
[3] *Photorefractive Materials and Applications I*, edited by P. Günter and J. -P. Huignard (Springer-Verlag, Berlin, 1988).
[4] A. A. Izvanov, A. E. Mandel, N. D. Khat'kov, and S. M. Shandarov, Avtometriya No. 2, 79 (1986) [Optoelectron. Data Process. Instrum. No. 2, 80 (1986)].
[5] S. I. Stepanov, S. M. Shandarov, and N. D. Khat'kov, Fiz. Tverd. Tela (Leningrad) **29**, 3054 (1987) [Sov. Phys. Solid State **29**, 1754 (1987)].
[6] P. Günter and M. Zgonik, Opt. Lett. **16**, 1826 (1991).
[7] M. Zgonik, R. Schlesser, I. Biaggio, E. Voit, J. Tscherry, and P. Günter, J. Appl. Phys. **74**, 1287 (1993).
[8] J. F. Nye, *Physical Properties of Crystals* (Clarendon, Oxford, 1957).
[9] D. Berlincourt and H. Jaffe, Phys. Rev. **111**, 143 (1958).
[10] A. Schaefer, H. Schmitt, and A. Dörr, Ferroelectrics **69**, 253 (1986).
[11] J. P. Remeika, J. Am. Chem. Soc. **76**, 940 (1954).
[12] O. Nakao, K. Tomomatsu, S. Ajimura, A. Kurosaka, and H. Tominaga, Appl. Phys. Lett. **61**, 1730 (1992).
[13] T. Ishidate and S. Sasaki, J. Phys. Soc. Jpn. **56**, 4214 (1987).
[14] S. Ducharme, J. Feinberg, and R. R. Neurgaonkar, IEEE J. Quantum Electron. **QE-23**, 2116 (1987).
[15] L. A. Shebanov, Phys. Status Solidi A **65**, 321 (1981).
[16] M. G. Cohen, M. DiDomenico, Jr., and S. H. Wemple, Phys. Rev. B **1**, 4334 (1970).
[17] R. W. Dixon and M. G. Cohen, Appl. Phys. Lett. **8**, 205 (1966).
[18] K. Buse, S. Riehemann, S. Loheide, H. Hesse, F. Mersch, and E. Krätzig, Phys. Status Solidi A **135**, K87 (1993).
[19] J. Sapriel, *Acousto-optics* (J. Wiley & Sons, Chichester, 1979).
[20] I. P. Kaminow, Appl. Phys. Lett. **7**, 123 (1965); **8**, 54E (1966).
[21] A. R. Johnston, Appl. Phys. Lett. **7**, 195 (1965).
[22] P. Jullien, A. Maillard, G. Ormancey, A. Lahlafi, and R. Matull, Ferroelectrics **94**, 81 (1989).
[23] P. Jullien, A. Lahlafi, A. Maillard, and G. Ormancey, Ferroelectrics **108**, 147 (1990).
[24] L. Holtmann, Ph.D. dissertation, FB Physik, Universität Osnabrück, Osnabrück, Germany, 1991.
[25] PROFIT 4.1, Quantum Soft, Postfach 6613, CH-8023 Zürich, Switzerland.
[26] W. H. Press, B. P. Flannery, S. A. Teukolsky, and W. T. Vetterling, *Numerical Recipes — the Art of Scientific Computing*, 2nd ed. (Cambridge University Press, Cambridge, 1992).
[27] M. Onoe, H. F. Tiersten, and A. H. Meitzler, J. Acoust. Soc. Am. **35**, 36 (1963).

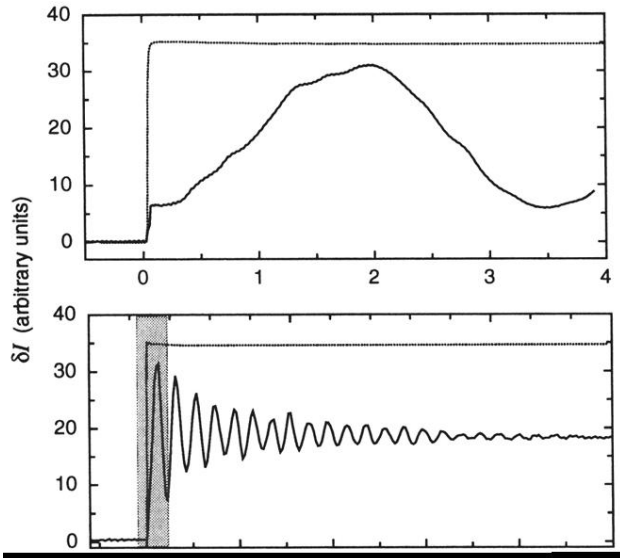

D_3 and the light polarization along the c axis. The quotient between the first step and the stationary value gives in this case the ratio $r^S_{333}/[r^T_{333} - 2(n_c - 1.5)d_{311}/n_c^3]$.